NUCLEAR INSTRUMENTS AND METHODS 31 (1964) 226–232; © NORTH-HOLLAND PUBLISHING CO.

CALIBRATION AND PERFORMANCE OF A NEUTRON-TIME-OF-FLIGHT DETECTOR†

J. B. CZIRR and D. R. NYGREN

University of Washington, Seattle, Washington

C. D. ZAFIRATOS

Los Alamos Scientific Laboratory, Los Alamos, New Mexico

Received 25 June 1964

The properties of a neutron detector for time-of-flight studies in the MeV energy region are described; calibration techniques for obtaining the absolute efficiency vs energy relationship are discussed and the results presented.

In addition, the pulse-height response of several organic scintillators under neutron irradiation was measured and compared to the pulse height obtained from a gamma-ray source.

1. Introduction

For time-of-flight studies in the MeV region, we have attempted to optimize in the design of a neutron detector the properties of high uniform detection efficiency, large solid angle, maximum light production and collection and good time resolution. Accordingly, several liquid and plastic scintillators have been investigated. As previously reported[1]), an efficient liquid scintillator using pseudocumene as the solvent[2]) has been found to have the following characteristics: yields 70% more light from five-MeV-alpha particles than the best plastic scintillators, has 7% greater hydrogen density than xylene or vinyl toluene, has a smaller absorption coefficient for its own light than polymerized plastics, and attacks lucite only very slowly.

In an effort to take advantage of these characteristics, a large-volume detector was built and calibrated at several energies with a known neutron flux.

The efficiency calibration was accomplished with a technique which removes the necessity of a beam monitor. An additional result of this program was the determination of the zero-angle neutron yield from the reaction Be^9 (d, n)B^{10*} for deuteron energies of 2.8, 3.1, 3.5 and 4.5 MeV, with as many as 10 levels of the residual B^{10*} nucleus observable. A measurement of the relative neutron yield from these levels provides a convenient calibration scheme for neutron time-of-flight detectors in the MeV region.

A subsidiary result of these measurements was the determination of the pulse-height response to neutrons of known energy for several organic scintillators. These results are presented in the form of curves giving the beta-ray energy which yields the same pulse height as the maximum-energy knock-on protons from the neutron irradiation.

† This work was supported by the National Science Foundation and by the U.S. Atomic Energy Commission.

2. Neutron-detector construction details

The liquid scintillator container consisted of a 3 × 6 × 12 in. polished lucite box with ¼ in. thick walls. This box was optically sealed on one 3 × 6 in. end to a 12-in. long lucite light pipe which in turn was sealed to a 5 in. phototube, the RCA 7046. The phototube end of the light pipe was octagonal in shape with a 3½ in. diameter inscribed circle. For this photomultiplier, variations in photoelectron transit times are significantly reduced by this restriction. The sides of the liquid con-

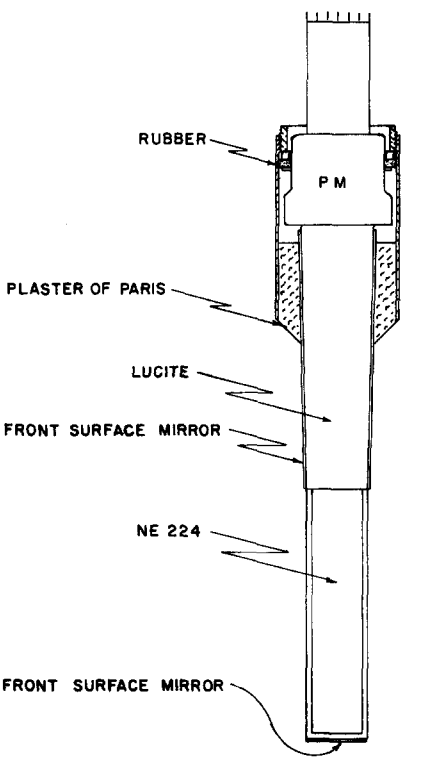

Fig. 1. Diagram of the neutron detector. The neutron beam is incident from the side.

tainer were loosely wrapped with specular Al foil and to the far end was attached a first surface evaporated Al mirror. The eight sides of the light pipe were also covered with Al mirrors in order to partially recover the loss (due to the factor of two decrease in cross-sectional area) in trapped light traversing the light pipe. The end mirror increased the amount of light reaching the phototube by 40%, and the eight side mirrors by 35%, for a total gain of 90% in pulse height.

The phototube, side mirrors and mu-metal shield were held in place by plaster of Paris and a brass sleeve as in fig. 1. A nitrogen bubble of about 1 cm diameter was introduced into the scintillator volume to relieve possible stresses from thermal expansion.

3. Experimental technique

The above detector was designed to be used in a time-of-flight experiment involving 1 to 4 MeV neutrons. The calibration was performed with the large Los Alamos Electrostatic Generator in conjunction with a Mobley-magnet ion buncher. This system has been described in detail in [3,4]). The source of neutrons was the reaction Be^9 (d, n) B^{10*}. For deuterons in the MeV region, as many as 13 states of the residual B^{10} nucleus are excited, yielding a wide range of neutron energies plus the corresponding de-excitation gamma-rays. A 100 $\mu g/cm^2$ Be target was bombarded with deuterons of energy 2.8, 3.1, 3.5 and 4.5 MeV. The resultant neutrons from the various levels were identified by their time-of-flight over a 4.33 m path.

The relative yield of the various neutron groups was measured with a small plastic-scintillator neutron counter which was calibrated from the known angular distribution of neutrons scattered from protons. Neutrons from the reaction T(p, n)He^3 impinged on a 10 g polyethylene cylinder and those scattered from protons in the sample were observed at angles corresponding to the energies of interest. The counting rate at an angle θ, divided by $\cos\theta$ yields the relative efficiency of the small counter. The smoothed curve representing the efficiency of this counter is shown in fig. 2.

This calibrated counter was then used to measure the time-of-flight spectrum under conditions similar to those used in the measurements on the large counter. Alternate data runs of target in-target out were taken at the same angle (0°) and deuteron energy, first with the large counter and then with the small calibrated counter. Because of the better time resolution and well shielded condition of the small counter, it was possible to obtain considerably more information about the detailed level structure of the B^{10*} nucleus with this detector. As many as 10 levels were clearly observed

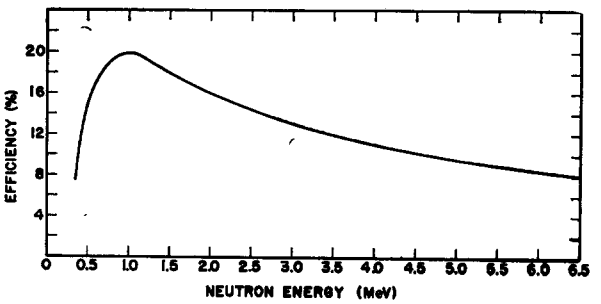

Fig. 2. Efficiency vs energy for a 1 in. thick plastic scintillator NE102. The absolute efficiency scale was determined with the aid of a long counter.

and the relative yields obtained at the four deuteron energies employed. Table 1 lists the results of these measurements along with the data obtained from the large counter and the resulting efficiency determined for the latter.

The neutron energies and level numbers quoted in table 1 were obtained from measurements of the excitation energy of the residual B^{10*} nucleus[5]). The stated errors include in all cases an estimate of the uncertainty arising from background subtraction. The data at each deuteron energy are normalized to that level for which the neutron energy is closest to 2 MeV, so that the relative efficiencies obtained from the large counter at the four deuteron energies may be combined into a single curve. It is necessary in doing this to calculate the efficiency over the energy region from 1.77 to 2.26 MeV. For the present bias level of approx. 0.4 MeV and a 2½ in. thick scintillator, the response varies less than 2% in the above energy region. As another example, for the 1 in. thick calibrated counter used to

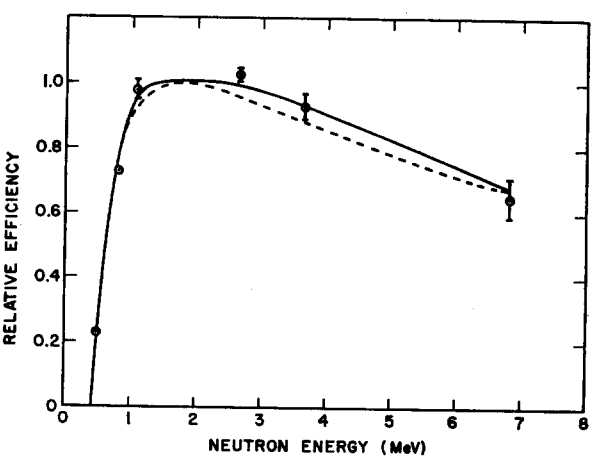

Fig. 3. Measured efficiency of the large liquid-scintillator counter. The dashed curve is based on a calculation assuming a bias level of 0.42 MeV. The solid curve represents an estimate of the line of best fit to the data.

TABLE 1

B^{10*} level	Neutron energy	Small counter eff.	Small counter counts	Relative yield at 4.33 m	Relative yield at source	Large counter counts	Relative eff.
			$E_d = 2.80$ MeV	$\theta = 0°$			
0	7.15 MeV	~ 7.7%	682	0.048	0.048 (7)	4 600	0.65
1	6.44	8.1	1 042	0.069	0.069 (7)		
2	5.42	9.1	296	0.017	0.017 (30)		
3	5.00	9.5	458	0.026	0.026 (15)		
4	3.55	11.8	1 436	0.066	0.066 (7)		
5	2.32	14.9	—	U	U		
6	1.96	16.0	29 630	1.000	1.000	60 066	1.000
7	1.91	16.3	—	S	S		
8	1.67	17.3	—	S	S		
9	1.45	18.1	—	S	S		
10	1.06	19.8	7 079	0.193	0.195 (3)	11 448	0.981
11	0.947	19.8	542	0.015	0.015 (30)		
12	0.781	19.0	747	0.021	0.021 (15)		
13	0.480	14.2	20 496	0.780	0.800 (3)	10 830	0.230
14	0.237	0	—	U	U		
			$E_d = 3.1$ MeV	$\theta = 0°$			
0	7.45	U	1 128	U	U		
1	6.74	~ 8.0%	1 283	0.064	0.064 (8)		
2	5.72	8.8	314	0.014	0.014 (30)		
3	5.30	9.2	345	0.015	0.015 (25)		
4	3.85	11.3	2 106	0.074	0.075 (10)		
5	2.61	14.1	—	U	U		
6	2.26	15.1	37 815	1.000	1.000	91 178	1.000
7	2.20	15.3	—	S	S		
8	1.97	16.0	—	S	S		
9	1.74	16.8	—	S	S		
10	1.36	18.6	8 779	0.188	0.189 (8)		
11	1.25	19.1	—	U	U		
12	1.09	19.8	—	U	U		
13	0.800	19.2	41 678	0.866	0.871 (2)	58 673	0.742
14	0.582	16.4	—	S	S		

measure the neutron yield, the relative efficiency varies 10% within this same energy region. A fairly complete calculation of the effect of the changing hydrogen and carbon cross sections plus the bias effect would be necessary in this case. An example of a calculation of this type is that of Hardy[6]), who was able to reproduce the relative change in a measured efficiency curve to within a few percent over a larger energy range.

A rough estimate of the relative B^{10*} level-six yield vs deuteron energy may be obtained using the integrated deuteron beam current as a monitor. The results are: 2.8 MeV-1.00, 3.1 MeV-1.09, 3.5 MeV-1.01, 4.5-MeV-1.04. These values should be reliable to $\pm$ 10%.

4. Calibration results

The efficiency of the large counter, shown in fig. 3, is seen to be constant to within 10% over the energy region from 1 to 4 MeV. The dashed curve of fig. 3 was obtained from a calculation which neglected the presence of carbon in the liquid scintillator. The effect of the narrow carbon resonances is found to be greatly suppressed in the $2\frac{1}{2}$ in. thick scintillator due to the high probability of second scattering from hydrogen after a primary carbon collision.

The bias level, determined by the 0.48 MeV point, is found to be at 0.42 MeV proton energy. From a measurement of the single electron pulse height of the RCA 7046 phototube, this bias is found to correspond to a pulse height of 4.7 photo-electrons. The dark current rate of the selected phototube was 140 counts per second at this level. A more typical rate for good tubes of this type under the same gain conditions is 600 counts per second.

An equation of the following form was used to obtain

TABLE 1 (*continued*)

B^{10}* level	Neutron energy	Small counter eff.	Small counter counts	Relative yield at 4.33 m	Relative ydiel at source	Large counter counts	Relative eff.
			E_d = 3.5 MeV θ = 0°				
0	7.86	U	719	U	U		
1	7.15	7.5%	964	0.269	0.264 (12)		
2	6.12	8.4	191	0.048	0.047 (30)		
3	5.70	8.8	430	0.10	0.10 (20)		
4	4.25	10.6	1 617	0.32	0.31 (10)		
5	3.00	13.0	—	U	U		
6	2.65	13.9	26 448	4.00	3.94 (2)	90 181	1.026
7	2.59	14.1	—	S	S		
8	2.37	14.7	—	S	S		
9	2.14	15.5	—	S	S		
10	1.77	16.8	8 032	1.000	1.000	22 220	1.000
11	1.65	17.2	525	0.064	0.064 (30)		
12	1.50	17.9	1 652	0.193	0.191 (12)		
13	1.23	19.2	56 429	6.15	6.05 (7)		
14	1.03	19.8	—	S	S		
			E_d = 4.5 MeV θ = 0°				
0	8.86	U	901	U	U		
1	8.14	U	—	U	U		
2	7.11	U	—	U	U		
3	6.67	U	—	U	U		
4	5.23	9.3%	—	U	U		
5	4.00	11.0	—	U	U		
6	3.65	11.6	22 429	0.837	0.842 (4)	66 768	0.941
7	3.59	11.7	—	S	S		
8	3.36	12.2	—	S	S		
9	3.13	12.7	—	S	S		
10	2.76	13.6	8 174	0.260	0.259 (6)		
11	2.65	13.9					
12	2.50	14.4	1 118	0.034	0.034 (50)		
13	2.23	15.2	35 130	1.000	1.000	84 822	1.000
14	2.03	15.9	—	S	S		

The symbol U represents an undetermined yield, usually because of a background subtraction problem. The symbol S represents a yield too small to be observed. A yield as great as $\frac{1}{2}$ of the smallest reported yield would probably have been detected. The numbers in parentheses in the sixth column are an estimate of the probable error in the corresponding yield. The measured yield at 4.33 m was corrected for air scattering to obtain the relative yield at source.

the dashed curve of fig. 3: $[1-\exp(\sum_H d)][1-0.42/E]$, where $\sum_H$ is the neutron-proton macroscopic cross section, $d = 2.5$ in. and E is in MeV. The bias effect given by the term $(1-0.42/E)$, is based upon the uniform probability per unit energy for knock on protons produced by neutrons. A reasonable fit is obtained from 0.5 MeV to 7 MeV, using this equation.

The absolute efficiency was determined at 1.0 MeV using mono-energetic neutrons from the reaction $T(p, n)He^3$, monitored by a calibrated long counter. The value obtained was 30%, with an estimated uncertainty of $\pm$ 3%.

From the knowledge of the bias level and the "fast" curve of fig. 7 (see section 5), one can obtain the number of detected photo-electrons at any knock-on-proton energy. This number varies from the lower limit of 4.7 photo-electrons to 160 photo-electrons at 4.0 MeV. The average time at which the half-maximum pulse height occurs for the RCA 7046 phototube was measured with a Tektronix 517A oscilloscope over this pulse-height region using a pulsed light source. A maximum time variation of 0.30 nsec was observed over the factor of 35 range in pulse height. Under the gain conditions chosen, systematic timing errors are seen to be small for flight times of the order of 100 nsec.

From the neutron peaks obtained during the calibra-

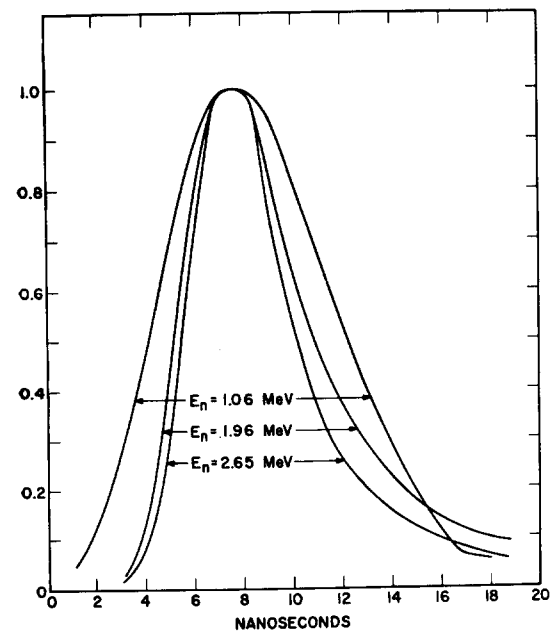

Fig. 4. Time of flight resolution at various neutron energies. The resolution at 3.65 MeV was similar to that at 2.65 MeV.

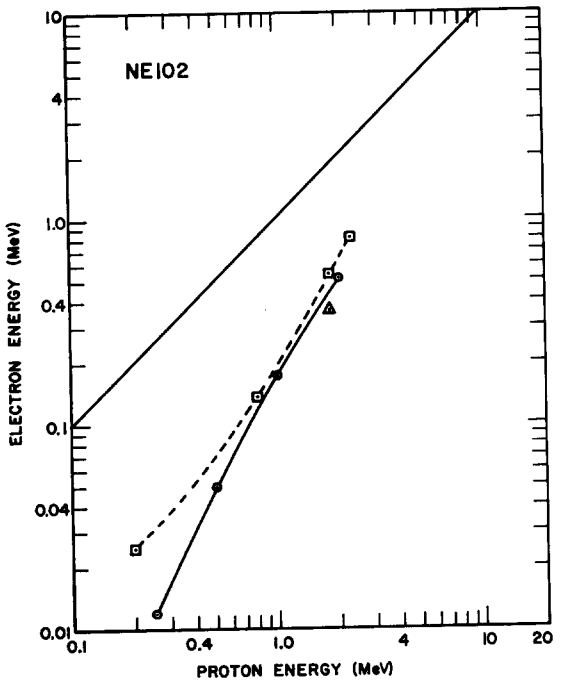

Fig. 5. Electron energy vs proton energy yielding equal pulse height for NE102 plastic scintillator. The dashed curve was obtained from ref. [9]), taken with an integrating time of 0.1 μsec. The solid curve is from the present work, with an integrating time of 1 μsec. The straight line represents the pulse height to be found with no quenching effect. The triangle represents the Po^{210} data.

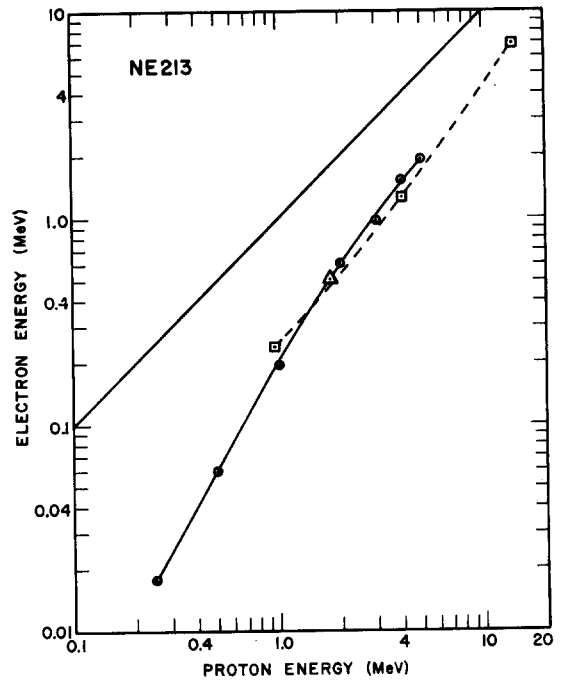

Fig. 6. Electron energy vs proton energy yielding equal pulse height for NE213 liquid scintillator. The dashed curve was obtained from ref. [10]), taken with an integrating time of 3 μsec. The solid curve is from the present work, with an integrating time of 1 μsec. The triangle represents the Po^{210} data.

tion runs, it is possible to determine the intrinsic timing resolution of the large detector. Representative time-of-flight peaks are shown in fig. 4. For these neutron energies, carbon scattering followed by hydrogen collisions produces the tail observed.

5. Scintillator comparison

The pulse-height distribution under neutron irradiation was determined for several organic scintillators using a pulse-height analyzer with an integrating time of approx. 1 μsec. The knock-on-proton energy loss for which the pulse height is equal to that of a beta particle of known energy loss was determined for each scintillater using a Cs^{137} source. The 0.477 MeV maximum-energy Compton electron was used to obtain what was assumed to be the linear relationship between beta energy and light output. For both the proton and electron spectra, the maximum pulse height was obtained from the half intensity value near the upper end of the differential spectrum. Mono-energetic neutrons were obtained from the reaction $Li^7(p, n)Be^7$ for 0.25, 0.50 and 1.0 MeV neutrons and $T(p, n)He^3$ for 1.0 MeV and above. The data for all scintillators were obtained with the same phototube and with all materials contained in glass bottles of the same dimensions. The plastic

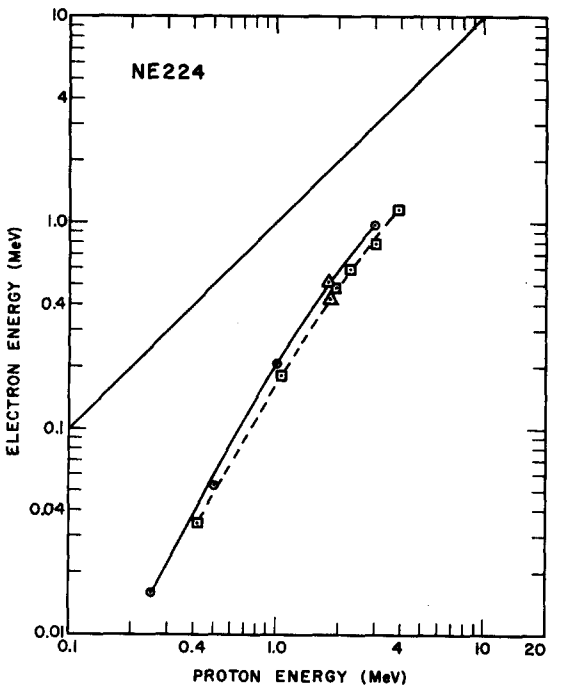

Fig. 7. Electron energy vs. proton energy yielding equal pulse height for NE224 liquid scintillator. The solid curve is from the present work, with an integrating time of 1 μsec. The dashed curve was taken with an integrating time of 5 nsec. The triangles represent the Po^{210} data, the upper point taken with an integrating time of 0.5 μsec, the lower with 5 nsec.

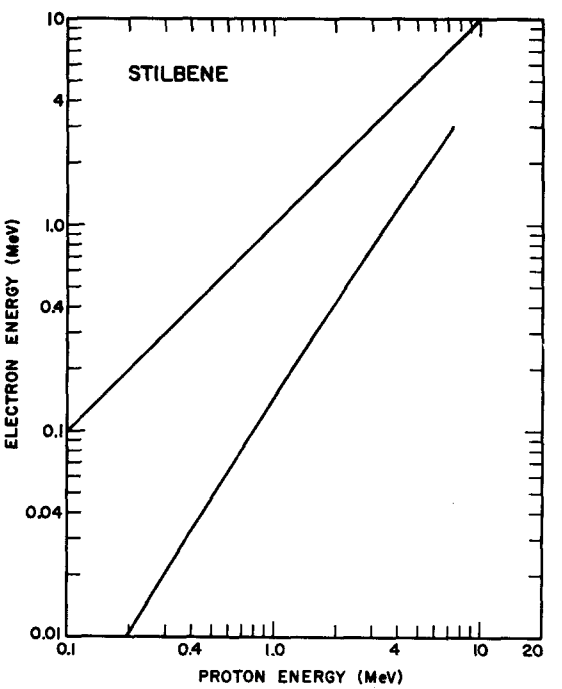

Fig. 8. Electron energy vs proton energy yielding equal pulse height for a stilbene scintillator. The data were obtained from the summary presented in ref. [7]). The integrating time was of the order of 1 μsec.

TABLE 2
Electron energy for equal pulse height

E_p	NE102 *slow*	NE213 *slow*	NE224 *slow*	Stilbene[7]) *slow*	NE102 *fast*	NE224 *fast*
0.25 MeV	0.012 MeV	0.018	0.016	0.0155		
0.42						0.035
0.50	0.050	0.060	0.053	0.047		
1.00	0.176	0.194	0.208	0.145		
1.06						0.181
1.96						0.485
2.00	0.517	0.603		0.420		
2.26						0.595
3.00		0.975	0.980	0.78		0.797
3.85						1.16
4.00		1.52		1.20		
5.00		1.91		1.67		
7.50				3.00		
1.8 MeV p	0.44	0.52	0.51			0.42
5.3 MeV α	0.38	0.52	0.52			0.43
Relative[1]) β ph	1.00	1.30	1.35	$\sim$ 1.0	1.00	1.43

The columns labeled *slow* represent data taken with an integrating time of the order of 1 μsec; the columns labeled *fast* represent a 5 nsec integrating time. The row labeled relative β ph has taken NE102 as a standard of pulse height, slow data to be compared to NE102 slow and fast data to NE102 fast. E_p is knock-on-proton energy. The discrepancy in alpha vs proton pulse height shown in column two is probably due to an error in the technique of ref. [1]) when applied to plastic scintillators, rather than a real variation in alpha vs proton energy for equal pulse height.

tested (NE102) was placed in optical contact with its bottle with mineral oil. Figs. 5 to 7 and table 2 show the results of these measurements, along with previously available data. It should be noted that the integrating time varies somewhat from measurement to measurement. However, the integrating time is large enough in most cases that the varying effect of decay time differences under proton irradiation and electron irradiation should be small. Fig. 8 is a plot of the stilbene data available as obtained from the summary given in [7]). These latter data are the results of many careful investigations and are presented to show the similarity of response of various organic scintillators when using a detection system with a long integrating time. In addition to the proton pulse height, figs. 5 to 7 show the results of equivalent pulse-height measurements using the 5.3 MeV alpha particles from Po^{210}, ref. [1]). The pulse height of alpha particles of this energy has been found, in anthracene crystals, to equal that of 1.8 MeV protons[8]). It is seen that reasonable agreement with the neutron data was obtained, particularly in the case of the liquids, indicating that a useful comparison of future scintillators can be made with the comparatively simple techniques described in [1]).

Also presented in fig. 7 is the result of a measurement of NE 224 response to neutron irradiation using a short integrating time on the phototube output. An integral discriminator curve was taken at each neutron energy using a tunnel diode discriminator with an integrating time of approx. 5 nsec, so that only the fast components of the scintillator light output were used to trip the discriminator. A Na^{22} gamma source was used to provide the linear beta response using the same technique. The pulse height was taken as the intercept of the extrapolated linear portion of the integral curves. Again in this case, Po^{210} data obtained with the same electronics show good agreement with the neutron data. The separation between the fast and slow curves is a measure of the pulse-shape-discrimination capability of NE224.

References

1) J. B. Czirr, Nucl. Instr. and Meth., **25** (1963) 106.
2) Available as NE 224 from Nuclear Enterprises, Ltd., 550 Berry St. Winnipeg, Canada. The solute concentrations were: p-terphenyl 4.5 g/l, POPOP 0.10 g/l.
3) L. Cranberg, R. A. Fernald, E. S. Hahn and E. F. Shroder, Nucl. Instr. and Meth., **12** (1961) 335.
4) L. Cranberg, J. S. Levin and C. D. Zafiratos, Bull. Am. Phys. Soc., **8** (1963) 82.
5) F. Ajzenberg-Selove and T. Lauritsen, Nucl. Phys., **11** (1959) 1.
6) J. E. Hardy, Rev. Sci. Instr., **29** (1958) 705.
7) B. V. Rybakov and V. A. Siderov, *Fast-Neutron Spectroscopy* (Consultants Bureau, Inc., 1960), p. 62.
8) F. D. Brooks, Prog. in Nucl Phys., **5** (1956) 278.
9) M. Gettner and W. Selove, Rev. Sci. Instr., **31** (1960) 450.
10) R. Batchelor, W. B. Gilboy, J. B. Parker and J. H. Towle, Nucl. Instr. and Meth., **13** (1961) 70.